



**INFN/AE-06/01**  
**5 Maggio 2006**

**OVERVIEW OF THE ELECTRICAL CHARACTERIZATION OF THE AMS/CMS  
SILICON MICROSTRIP DETECTORS**

Nicoleta Dinu<sup>1,\*</sup>, Emanuele Fiandrini<sup>1</sup>, Livio Fanò<sup>1</sup>

<sup>1</sup>*INFN-Sezione di Perugia, Via A. Pascoli, 06123, Perugia, Italy*

**Abstract**

This paper presents an overview of the electrical parameters commonly measured for the electrical certification of silicon micro-strip sensors. Mainly, parameters which contribute to the noise at the input of the read-out electronics will be described: the single-strip leakage current, the biasing resistance (the poly-silicon resistance for poly-silicon biasing and the bias-ring to strip resistance for punch-through biasing), the dielectric current and the coupling capacitance (for AC-coupling). Global parameters like total capacitance and total leakage current will be also presented. The general characteristics of the hardware system and a description of the electrical set-up configurations recommended for an accurate measurement of the electrical parameters will be also illustrated.

PACS.: 29.40Gx, 29.90.+r

*Poster at the 10<sup>th</sup> European Symposium on Semiconductor Detectors, Wildbad Kreuth,  
June 12-16 2005*

*Published by SIS-Pubblicazioni  
Laboratori Nazionali di Frascati*

---

\* On leave from Institute of Space Sciences, Bucharest, Romania

## 1 INTRODUCTION

Many particle detectors use silicon tracker systems to measure the particle parameters. These systems are among the most sensitive, high precision tracking devices. Challenging features are also compactness in size, very fast response time, low power consumption, good operation in vacuum, strong magnetic fields and high radiation hardness. All these characteristics make them very suitable for high radiation environments in particle accelerator experiments (e.g. CMS, LHCb, ATLAS, ALICE at LHC p-p collider at CERN – Switzerland; CDF and D0 at Tevatron p-antiproton collider at FNAL – USA; BABAR, CLEO, BELLE at B-factory colliders at SLAC and Cornell – USA and respectively KEK - Japan; H1 and ZEUS at HERA e-p collider at DESY – Germany) as well as in space experiments (e.g. AMS, GLAST, PAMELA, AGILE).

The particles detection efficiency and the spatial resolution of silicon trackers depend strongly on the electrical parameters of their basic element, the silicon micro-strip sensor. These electrical parameters are very important because they contribute to the noise at the input of the read-out electronics and hence influence the performances of the tracker system. Therefore, to obtain the best possible signal-to-noise ratio and to guarantee the quality of the data taken with silicon tracker systems during the whole experiment running, a very accurate electrical characterization of the silicon micro-strip sensors must be performed prior their final assembly.

The aim of this paper is to give an overview of the electrical parameters commonly measured for the electrical certification of silicon micro-strip sensors. This overview is essentially based on the experience accumulated during electrical characterization of silicon micro-strip sensors fabricated for two selected experiments having large silicon tracker systems: the Compact Muon Solenoid (CMS)<sup>1)</sup> - future experiment at LHC accelerator at CERN and the Alpha Magnetic Spectrometer (AMS-02)<sup>2)</sup> – future astrophysics experiment on International Space Station. The general characteristics of the hardware system and a description of the electrical set-up configurations recommended for an accurate measurement of the electrical parameters will be also presented.

## 2 GENERAL DESCRIPTION OF THE MICRO-STRIP SENSORS

The silicon micro-strip sensors are usually made from n-type silicon wafers grown by Float-Zone technique (the most suitable for detector-grade silicon with respect to the Czochralski growth method widely used for microelectronics applications). The silicon wafers have high resistivity ( $1\div 10$  k $\Omega$ cm) and are cut with  $\langle 111 \rangle$  or  $\langle 100 \rangle$  lattice orientation as a function of the experiment requirements (e.g.  $\langle 100 \rangle$  orientation is preferable for particle accelerator experiments because it gives better performances after irradiation with respect to the standard  $\langle 111 \rangle$  orientation<sup>3)</sup>). The wafers have usually a thickness of  $\sim 300$   $\mu$ m ( $\sim 500$   $\mu$ m is also used) and are processed by planar technology (adapted to detector fabrication by Kemmer in 1980<sup>4)</sup>) which allows high-resolution segmentation of silicon surface. The area of the sensors is variable and it is usually limited by the standard dimension of silicon wafers

used in industry, dimension which grown in the last years from 4” (~10 cm diameter) to 6” (~15 cm diameter).

A single-sided micro-strip sensor is realized segmenting one side of a silicon wafer in parallel strips, each strip representing a p-n junction obtained by a high-doping p<sup>+</sup> implant in the n-bulk. The distance between the strip centers (the pitch) can vary from 25 μm (giving high spatial resolution) to 200 μm (for applications where ultimate precision position is not required). On the other side of the wafer a high-doping n<sup>+</sup> implantation is performed to provide the ohmic contact to bias the detector. The side containing the strips is called for convenience the p-side (or diode side) and the opposite side is called the ohmic side.

The originally single-sided sensors had the p-strips directly coupled (DC) to the read-out electronics. Such method has the inconvenience that the leakage current of each strip has to be absorbed by the electronics. This does not in general affect the spatial resolution as long as the leakage current for a single strip remains bellows a certain value (~200 nA/strip). However, to avoid large dynamic range of the ADC’s converters required by this method, a new read-out method called capacitive coupling (AC) was developed<sup>5, 6</sup>. This method implies the presence of an insulating layer of SiO<sub>2</sub> (sometimes in combination with Si<sub>3</sub>N<sub>4</sub>) between the strip implant and the corresponding metallization. In this case only the AC part of the strip current reaches the electronics (an obvious advantage of shielding the electronics from the leakage current), while the DC part goes into the bias circuit.

A double-sided sensor is obtained segmenting the ohmic side of a single-sided sensor in strips which are obtained by high-doping n<sup>+</sup> implants and are usually set at 90 degrees relative to the p-side strips (for convenience this is called n-side). For double-sided sensors, the insulation of each of the strips from the others is quite difficult because the electron surface accumulation layer at the Si-SiO<sub>2</sub> interface would short-circuit the n<sup>+</sup> strips. The most frequently used method to disrupt the electron layer and to insulate the n<sup>+</sup> strips from each other is to surround them with high dose p<sup>+</sup> blocking rings (so-called p-stop design)<sup>7</sup>.

The bias voltage is carried uniformly to all the strips from a common bias line surrounding the strips (called bias-ring) through poly-silicon resistances or punch-through method.

The poly-silicon biasing<sup>5, 6</sup> represents the first biasing method successfully implemented in the fabrication of the single-sided sensors and it implies an array of poly-silicon resistors which connects the metal line of the bias-ring to one end of each strip. This method is usually used for single-sided sensors and it is also preferable for sensors used in particles accelerators experiments because of its well known radiation resistance<sup>8</sup>.

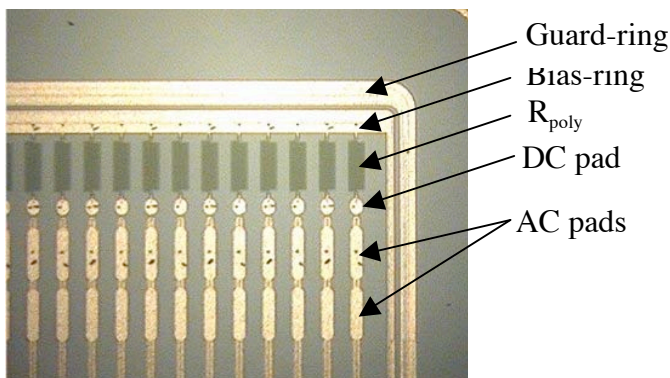
The punch-through biasing method<sup>9, 10</sup> is based on the fact that a voltage drop of few volts is established between the strips and the bias-ring if they are at few diffusion lengths away. This works both for p-n-p and n-p-n types. The voltage drop usually depends on the sensor geometry (a distance of few microns is required between the bias-ring and the end of the strips), the doping concentration and the bias voltage. This biasing method is simpler (it eliminates the additional technological steps required by poly-silicon resistors fabrication) and it is usually used for fabrication of double-sided sensors. It can, however, be only recommended for low radiation doses<sup>11</sup>.

The bias-ring is further surrounded by one (or more) guard-rings designed to reduce the surface leakage currents and to assure continuous potential drop over the edge region.

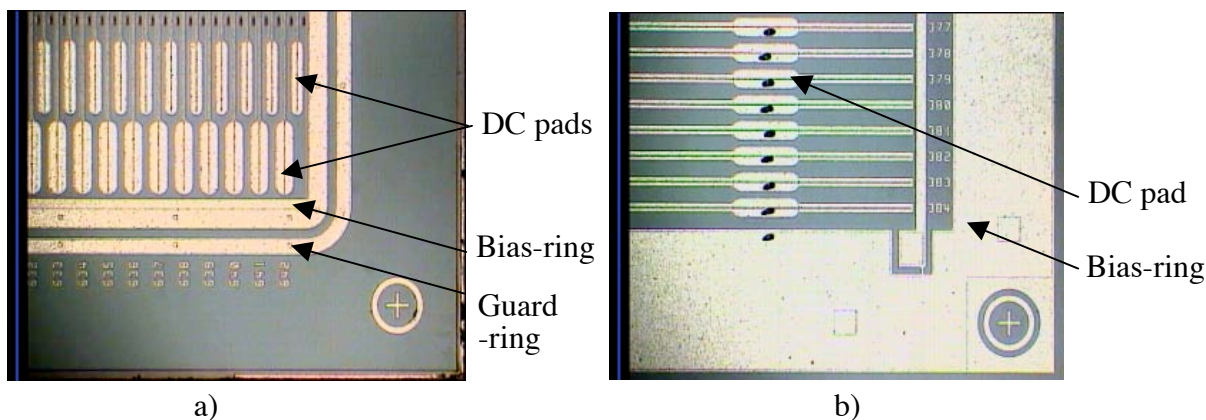
Generally, the selection of sensor design follows the physics requirements of the experiment. Few of the most important criteria for micro-strip sensors optimization are the position-measurements precision, the efficiency of the charge collection, the stability of the device and its radiation hardness.

Fig.1 presents a photograph of the corner of the CMS sensor. It represents an example of single-sided sensor used in an accelerator experiment having the  $p^+$  strips AC-coupled to the read-out electronics and biased through poly-silicon resistance (a detailed description of the CMS sensors design can be found in the reference<sup>12</sup>).

Two photographs of a corner of both p- and n-side of the AMS sensor are presented in Fig.2a) respectively Fig.2b). It is an example of double-sided sensor used in space physics experiment (where low-mass limitation frequently determines the technical design choice) having the strips biased through punch-through method (note the small distance between the bias-ring and the end of the strips on both sides). A detailed description of the AMS sensor design can be found in the reference<sup>13</sup>).



**FIG.1:** Photograph of a corner of single-sided sensor used by the CMS experiment. The sensor has  $p^+$  strips AC-coupled to the read-out electronics and biased through poly-silicon resistances



**FIG. 2:** Photograph of a corner of the p-side (a) and of the n-side of a double-sided sensor used by the AMS experiment. The strips are DC-coupled to the read-out electronics and punch-through biased. The n-side strips are set to 90 degrees with respect to the p-side strips

### 3 GENERAL REQUIREMENTS ON THE HARDWARE SET-UP

The electrical characterization of silicon micro-strip sensors requires stringent conditions on the measurements equipment. Mainly, such a system has to permit electrical measurements with at least 10% accuracy for current levels ranging from  $O(100\text{pA})$  to  $O(10\text{mA})$ , resistances of  $O(10\text{G}\Omega)$  to  $O(\text{T}\Omega)$  and capacitances down to  $O(\text{pF})$  with reproducible results immediately interpretable. Also, it is useful to have an automated system for a fast quality control of a large number of sensors in short time. To avoid the influence of contamination factors, the measurements have to be performed in a clean-room, with controlled temperature and humidity (usually  $21 \pm 1^\circ\text{C}$ ,  $35 \pm 5\% \text{RH}$ ).

As an example of such measurement equipment, Fig.3 illustrates the set-up used for the electrical characterization of both CMS and AMS silicon sensors in the class 1000 clean-room of INFN, Perugia Section, Italy. This system is made by the PA200 Karl Suss automatic test-station, instruments with adequately characteristics for measurements of semiconductor parameters as indicated before and a PC which provides the control of PA200 station and all instruments through a serial port and GPIB interface respectively.

The PA200 Karl Suss test-station is an example of an automatic system that allows the electrical characterization of one side of 25 sensors without interruption. It is flexible and can be used for different geometries of silicon micro-strip sensors, regardless of strip pitch and size of the sensors. The main elements of such system are the following:

- a storage cassette (1) – used for loading of the sensors; it is made from teflon to avoid damaging of the surface sensors;
- a pneumatic arm (2) – allows the automatic loading and unloading of the sensors;
- a chuck (3) – holds the sensors during the measurements; vacuum circuits of different diameters (2 or 5 cm - as a function of sensor dimension) are used to fix the sensors on the chuck;
- a probe-card (4) with variable number of needles – allows the connection between the metallized pads of the sensor strips and the instruments (the distance between needles corresponds to the pitch of the micro-strip sensors). The needles are usually made from tungsten and have rounded tips of  $10 \div 12 \mu\text{m}$  diameter. Two separate needles (placed on the chuck stage of the test-station) are used for biasing of the sensors. A connector (pin numbers equals the number of both probe-card and biasing needles) assures the connection between the needles and the corresponding triaxial cables connected to the measuring instruments;
- a microscope (5) and a video-camera (6) – assure an automatic alignment of the sensors with respect to the x-y axes of the chuck through an optical pattern-recognition system;
- an opaque Faraday box (7) – to avoid the photo-production of electron-hole pairs during electrical measurements.

Fig.3 shows a typical set of instruments used for the measurement of the electrical parameters of silicon micro-strip sensors:

- Keithley Vsource 230 (8) – voltage source which provides a voltage up to 100 V;

- Keithley IV 236 (9) and IV 237 (10) – precision source measure units (SMU) supplying voltage whilst measuring current or vice-versa. They can deliver a potential difference across terminals in the range  $-110\text{ V}$  to  $+110\text{ V}$  (model IV 236) or in the range  $-1100\text{ V}$  to  $+1100\text{ V}$  (model IV 237). The ammeter and the voltmeter of these instruments have nominal sensibility of  $10\text{ fA}$  and  $10\text{ }\mu\text{V}$ , respectively. One useful feature of these instruments is their compliance facility that is installed to protect the circuitry of the sample under test. This is accomplished, when applying a voltage source, by setting the compliance limit which sets the maximum current output level;
- Keithley CV-590 (11) – measures the capacitance and conductivity at high frequencies (100 KHz and 1 MHz) with a precision of 1fF; it includes also a voltage supply that can apply voltage up to 20V;
- Agilent 4284A (12) – gives the possibility of capacitance measurements in the frequency range (20 Hz ÷ 1 MHz);
- Keithley switching matrix SM-707 (8x72 channels) (13) – allows automatic multiplexing of many different electrical combinations through adequate switches.

To avoid dangerous ground loops, the chassis of each instrument is connected to the same ground as the Faraday box. The electrical connection between the instruments and the probe-card is performed by ground-shielded triaxial cables. Such a configuration assures low stray currents ( $I_{\text{open circuit}} \approx 10^{-12} \div 10^{-13}\text{ A}$ ) and low capacitive effects ( $\sim 1\text{ pF}$ ).

A PC running LabView programs is usually used to provide control of the test-station and all instruments and to record and analyze the electrical characteristics of the sensors.

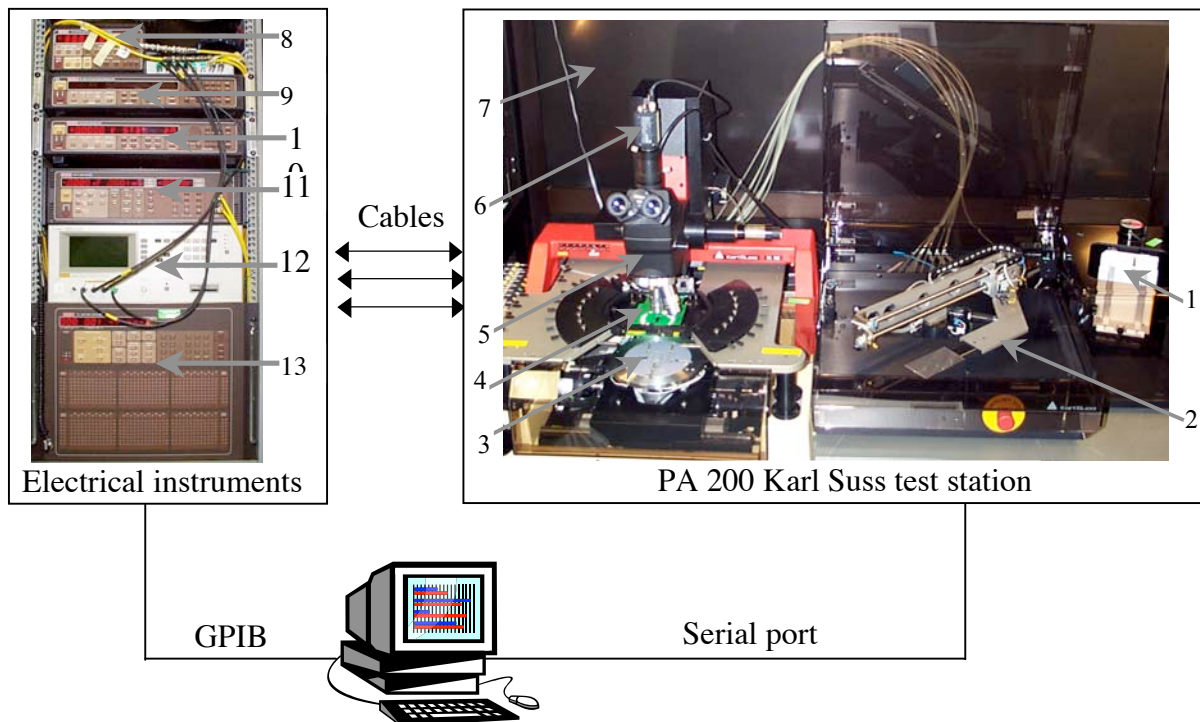


**FIG. 3:** Example of hardware set-up for the electrical characterization of silicon micro-strip sensors

#### 4. ELECTRICAL CHARACTERIZATION

For an efficient charge collection in a silicon micro-strip sensor, the signal given by a traversing minimum ionizing particle (MIP) should be much higher than the noise at the input of the read-out electronics.

The average energy loss per traversed length of a MIP in silicon is  $(dE/dx)_{Si} = 3.88$  MeV/cm. Therefore, the average energy loss in a 300  $\mu\text{m}$  thick silicon is  $\sim 116$  KeV. For the silicon sensors, usually is used the most probably energy loss of the Landau distribution ( $\approx 0.7 \times$  average energy loss)<sup>14)</sup>. Considering that  $\sim 75$  e-h pairs/ $\mu\text{m}$  are generated, the most probably charge deposition of a MIP traversing a typical thickness of  $\sim 300$   $\mu\text{m}$  of silicon sensor is  $\sim 22500$  e ( $3.6$  fC)<sup>15)</sup>. Therefore, the noise should be as low as possible than this value.

The noise represents any undesired fluctuation that appears superimposed on a signal source and its value is often expressed in terms of equivalent noise charge (ENC). In the complex case of a silicon tracker system, both silicon sensor and read-out electronics give noise contributions.

For the most used charge sensitive preamplifier, the main noise sources at the input of the read-out electronics are:

- the capacitive load, representing the principal source; the ENC referring to this contribution can be expressed by the formula:

$$ENC = a + bC \quad (1)$$

where a, b are constants depending of the preamplifier design and C is the capacitance of the strip being read-out;

- the sensor leakage current; for a simple CR-RC filter, the ENC referring to this contribution is given by<sup>16)</sup>:

$$ENC = (e/q) \sqrt{qIT_p/4} \quad (2)$$

where e is the natural logarithm base, q is the electron charge, I is the leakage current of the strip being read-out and the  $T_p$  is the peaking time, equal to the integration time of the shaper;

- the resistance of the bias resistor; the ENC contribution of the bias resistor can be calculated from the following expression:

$$ENC = (e/q) \sqrt{T_p \cdot kT/2R} \quad (3)$$

with k being the Boltzmann constant, T the temperature and R the biasing resistance of the strip.

As can be observed from the previous expressions, the electrical parameters of silicon micro-strip sensor give important noise contributions. Therefore, the relevant quantities required to be measured and analyzed for the electrical certification of the silicon micro-strip sensors are those which essentially give contribution to the noise of the corresponding read-out electronics channels:

- the leakage current of every strip for the shot noise contribution;
- the biasing resistor (the polysilicon resistance for the poly-silicon biasing and the resistance from the bias-ring to the strips for the punch-through biasing) which determines the bias parallel resistance noise;
- the current through the dielectric layer and the coupling capacitance (for AC-coupling) which identifies pinholes;
- the interstrip capacitance (for both DC and AC coupling) which determines the capacitive noise;
- the interstrip resistance which determines the DC electrical insulation.

A description of the first three parameters and examples of the electrical set-up configurations recommended for their accurate measurement will be illustrated in the following sections.

The interstrip capacitance and the interstrip resistance depend essentially on the geometry of the strip, the length and the width of the implantation and the aluminization. Taking into account that such parameters are well controlled during fabrication, their measurement is not mandatory for each sensor and the description of their measurement procedure is not a subject of this article. For such description the reader is referred to the work<sup>17)</sup>.

## 4.1 Global parameters

Before the analysis of the indicated single-strip parameters, the electrical characterization of a silicon micro-strip sensor requires the study of the following global parameters: the total capacitance (often named back-plane capacitance or bulk capacitance  $C_b$ ) and the total leakage current  $I_{tot}$ . The  $C_b$  allows the calculation of the depletion voltage  $V_d$  and the rough check of the thickness and the resistivity of the wafer crystal. The  $I_{tot}$  allows the study of the breakdown performances and it represents also a fairly good indicator of the quality of the sensor.

### 4.1.1. Total capacitance

To assure maximum charge collection efficiency, the silicon micro-strip sensors are operated in overdepleted mode: across the active volume of the sensor a reverse bias voltage  $V_{bias}$ , usually 1.5 or 2 times higher than the  $V_d$ , is applied. Therefore, to operate the sensors one has to determine a priori the voltage at which they deplete.

The depletion width  $w$  of a p-n junction is a function of the bulk resistivity  $\rho$ , charge carrier mobility  $\mu$  and the magnitude of the  $V_{bias}$ :

$$w \cong \sqrt{2\varepsilon\varepsilon_0\rho\mu V_{bias}} \quad (4)$$

where  $\varepsilon$  is the dielectric constant of the silicon,  $\varepsilon_0$  is the permittivity of the free space, and  $\rho$  is the bulk resistivity of the doped silicon expressed by:

$$\rho = 1/e\mu N \quad (5)$$

where  $e$  is the electron charge and  $N$  is the doping concentration.

The voltage needed to completely deplete a junction of thickness  $d$  is called depletion voltage  $V_d$ :

$$V_d = d^2/2\varepsilon\varepsilon_0\rho\mu \quad (6)$$

It is observed from this expression that a higher voltage is needed to deplete both low resistivity and p-type bulk material (the carrier mobility of holes is lower than for the electrons: 450 vs 1350 cm<sup>2</sup>/Vs). Therefore, as was noted in the Section 2, n-type bulk silicon with high resistivity is usually used for the fabrication of the silicon micro-strip sensors.

Since the capacitance of a p-n junction is simply the parallel plate capacity of the depleted zone, it depends on the  $V_{bias}$  through the following expression<sup>18</sup>:

$$C = A\sqrt{\varepsilon\varepsilon_0/2\rho\mu V_{bias}} \quad (7)$$

where  $C$  is the capacitance and  $A$  is the area of the junction. This expression shows that the junction capacitance decreases with increasing of the  $V_{\text{bias}}$  reaching a limiting value when the depth of the depleted zone equals the thickness of the sensor (further increase of the  $V_{\text{bias}}$  will not increase the charge). Rewriting the above expression as:

$$1/C^2 = 2\rho\mu V_{\text{bias}} / \epsilon\epsilon_0 A^2 \quad (8)$$

shows that  $1/C^2$  is linearly dependent on  $V_{\text{bias}}$  if  $V_{\text{bias}} < V_d$  and the limiting value is  $C_b = \epsilon\epsilon_0 A/d$  (total capacitance) for  $V_{\text{bias}} \geq V_d$ .

The  $V_d$  is determined experimentally measuring the  $C_b$  versus reverse  $V_{\text{bias}}$ . An example of the electrical set-up used for the measurement of the CV curve of a single-sided sensor is presented in Fig.4. The  $C_b$  is measured between the bias-ring and the back-plane of the sensor, keeping the guard-ring floating. A typical example of the  $C_b$  vs  $V_{\text{bias}}$  curve for a sensor is presented in Fig.5a). The  $V_d$  is extracted from the fit of the knee in the plot  $1/C_b^2$  versus  $V_{\text{bias}}$  as is shown in Fig.5b).

For the case of the CMS tracker, sensors with a thickness of 320  $\mu\text{m}$  and a resistivity of 1.5  $\div$  3.0  $\text{k}\Omega \text{ cm}$  were chosen for the inner layers (situated at distance of 20  $\div$  60 cm from the collision point in the radial direction), while sensors with 3.5  $\div$  7.5  $\text{k}\Omega \text{ cm}$  resistivity and 500  $\mu\text{m}$  thickness were used for the outer layers situated farther than collision point (60  $\div$  110 cm in the radial direction). The low resistivity and the thickness of the inner layers was chosen as a compromise between signal-to-noise ratio and full depletion voltage after irradiation expected during 10 years of LHC running. The requirements on the resistivity and the thickness were such that every sensor should deplete between 100 and 300 V.

For the case of AMS tracker, sensors with a thickness of 300  $\mu\text{m}$  and a resistivity  $>$  6  $\text{k}\Omega \text{ cm}$  were used. The depletion voltage of AMS sensors fulfilled the requirement to be less than 50 V.

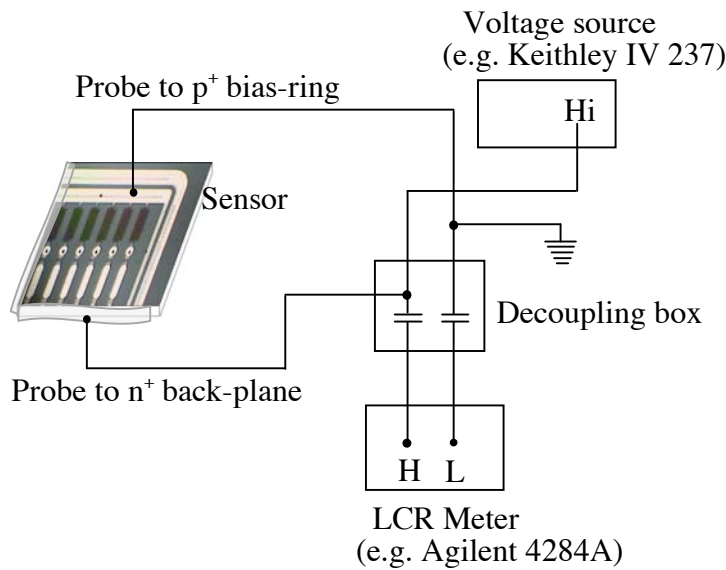


**FIG. 4:** Example of electrical set-up configuration for the measurement of the CV characteristic of a single-sided sensor

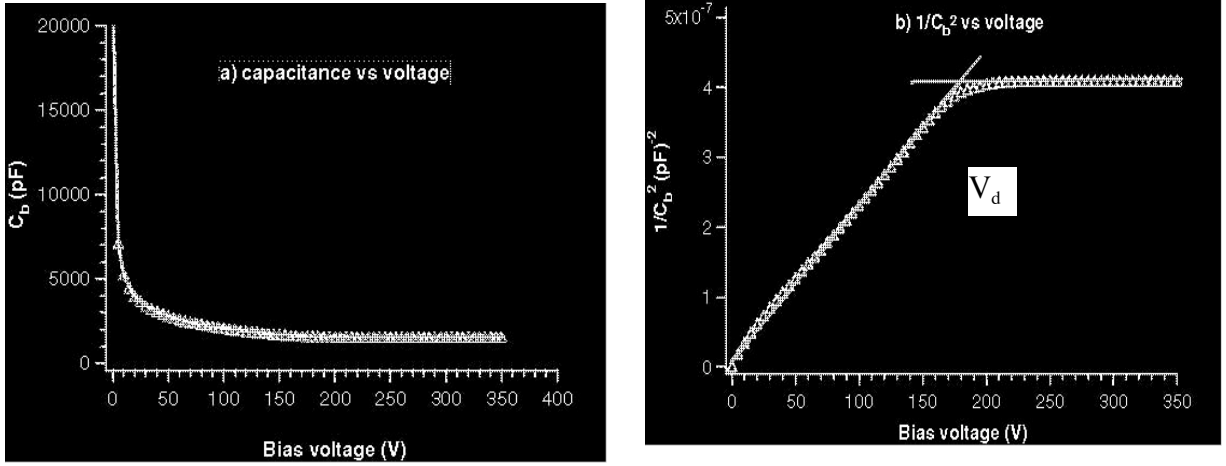


**FIG. 5a):** Typical  $C_b$  curve vs  $V_{bias}$ ; **b)** typical  $1/C_b^2$  curve vs  $V_{bias}$ ; the intersection of the two linear fits defines  $V_d$

#### 4.1.2. Total leakage current

To understand the sources of the leakage current in a silicon micro-strip sensor, one should refer to the properties of the p-n junction.

Even in the absence of ionizing radiation, some finite conductivity and therefore a small current (named leakage current) is observed when a reverse bias voltage is applied to a p-n junction. The origin of this leakage current is related to both bulk and surface of the junction.

The bulk leakage current has two main sources.

The first one is the diffusion current, determined by the minority carriers which diffuse into the depletion region from the adjacent un-depleted regions. This contribution should be negligible in a fully depleted silicon micro-strip sensor due to very small un-depleted regions.

The second source is the generation current, determined by thermal generation of electron-hole pairs in the depletion region from defects and contaminants. It has an exponential dependence of temperature:

$$J_g \propto \exp((-b)/kT) \quad (9)$$

where  $b$  is a constant,  $k$  is the Boltzmann constant and  $T$  is the temperature and its rate is determined by the nature and the concentration of defects. The sources of high generation currents can be non-uniformities produced during fabrication processes (e.g. defective implantations) as well as bulk crystal defects. Improper dicing of the device from the wafer can produce mechanical breakthrough, even invisible by naked eye inspection and such defects could also represent a source of generation current. The generation current represents

the major contribution to the leakage current of a silicon micro-strip sensor and therefore, low defects devices are desirable.

The surface leakage effects usually take place at the edges of the device where a voltage drop usually exists between the bias-ring and the edge. In the case of silicon micro-strip sensor, such surface contributions are minimized maintaining a proper distance (hundreds of  $\mu\text{m}$ ) between the bias-ring and the edge of the sensor. The presence of one or more guard-rings (often left floating) surrounding the bias-ring helps also to assure continuous potential drop over edge region. Sometimes an n-type implant around the edge of the sensor is also used to minimize the edge effect<sup>12)</sup>.

The global current parameter usually measured for the case of a silicon micro-strip sensor is the total leakage current  $I_{\text{tot}}$ . It represents essentially the algebraic sum with the corresponding signs of all the contributions mentioned before and is equal with the current in the sensor's bias-ring. Thanks to the resistive coupling of the strips to the bias-ring, the  $I_{\text{tot}}$  can also be interpreted with a good approximation as a sum of single strip leakage current contributions.

For the analysis of  $I_{\text{tot}}$ , one experimentally measures the dependence of  $I_{\text{tot}}$  as a function of reverse  $V_{\text{bias}}$ . An example of the electrical set-up and a typical IV curve for a CMS sensor are presented in Fig.6 respectively Fig. 7.

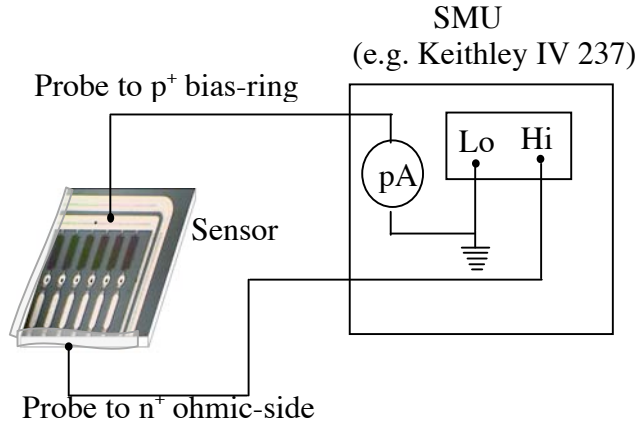


**FIG. 6:** Example of electrical set-up configuration for the measurement of the IV characteristic of a single-sided sensor

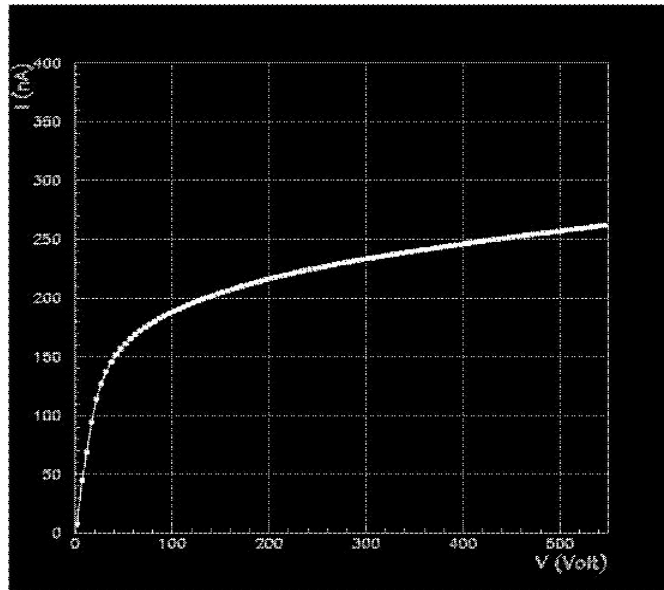


**FIG. 7:** Typical  $I_{\text{tot}}$  vs  $V_{\text{bias}}$  curve for a CMS single-sided sensor produced by Hamamatsu Photonics (300  $\mu\text{m}$  thickness, 768 strips, 6.15 x 11.68  $\text{cm}^2$  area)

As stated earlier, to assure maximum charge collection efficiency, a silicon micro-strip sensor works in over-depletion mode. There is, however, one key factor which imposes an upper limit on reverse bias voltage: the breakdown phenomenon (the avalanche multiplication or the impact ionization of host atoms by charge carriers in the high electric field regions). The critical voltage at which the reverse current through a junction increases sharply and relatively large currents can flow with small increase in voltage is called breakdown voltage  $V_{\text{br}}$ . Comparison between  $I_{\text{tot}}$  vs  $V_{\text{bias}}$  curves for micro-strip sensors with and without breakdown phenomenon are presented in Fig.8.

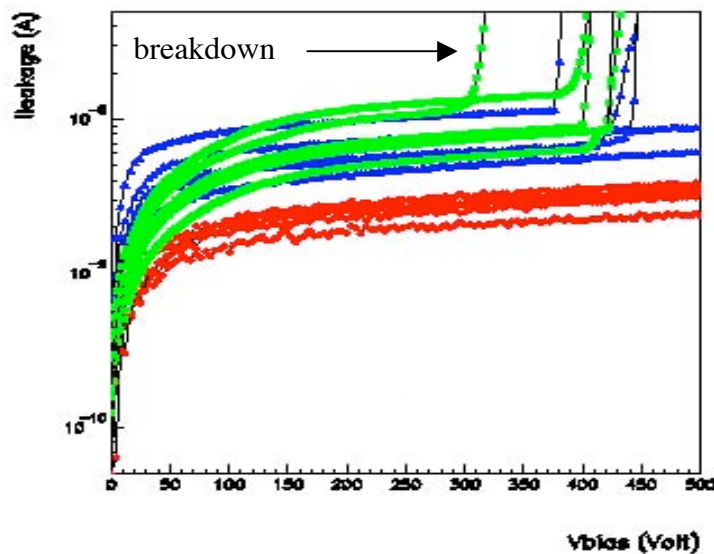


**FIG. 8:** Comparison between IV characteristics for micro-strip sensors with and without the breakdown phenomenon for bias voltages up to 500 V

The breakdown phenomenon usually occurs around  $30 \text{ V}/\mu\text{m}$  (typical operating field is less than  $1 \text{ V}/\mu\text{m}$ ). Local defects and inhomogeneities could result in fields approaching the breakdown limit. The breakdown can occur through the bulk as well as at the edge regions (surface breakdown) and also between any structures with sufficiently different potentials. Good sensors design (edge regions and structure dimensions) as well as high quality processing are needed to avoid breakdown problems.

Usually, the  $I_{\text{tot}}$  is requested to be less than a certain value at operating  $V_{\text{bias}}$ . For example, the upper limit for a CMS sensor is  $100 \div 150 \text{ nA}/\text{cm}^2$  depending on the sensor surface (equivalent with  $10 \mu\text{A}$ ) at  $V_{\text{bias}} = 450 \text{ V}$  and for an AMS sensor is  $70 \text{ nA}/\text{cm}^2$  (equivalent with  $2 \mu\text{A}$ ) at  $V_{\text{bias}} = 90 \text{ V}$ . Sensors with  $I_{\text{tot}}$  higher than limit values or presenting breakdown phenomenon are usually rejected.

## 4.2 Strip-by-strip electrical parameters

The single strip measurements require long time, depending of the number of strips to be tested for each sensor. Consequently they are usually performed contacting simultaneously a certain number of strip pads (using the probe-card) and automatically switching between different measurements.

During all measurements presented in the following, the sensor is maintained overdepleted: the  $V_{\text{bias}}$  applied between the  $p^+$  bias-ring and the  $n^+$  ohmic-side (or between  $p^+$  and  $n^+$  bias-rings for a double-sided sensor) should be higher than  $V_d$  of the sensor. The applied  $V_{\text{bias}}$  usually corresponds to operating bias voltage of the sensor during experiment running (1.5 or 2 times higher than  $V_d$ ).

### 4.2.1 Single-strip leakage current

In a silicon micro-strip sensor, high single-strip leakage currents  $I_{\text{ss}}$  may appear due to both local fabrication defects (e.g. small imperfections occurred during some process steps as for example chemical etchings or photolithography) as well as due to manipulations damages from dicing and transport (e.g. chipping, scratches). To minimize the number of noisy channels, it is mandatory to check that only a minimum number of the strips have current above a critical limit. For example, the upper limit requested for the  $I_{\text{ss}}$  of a CMS sensor is  $430 \text{ pA}/\text{cm}$  per  $\mu\text{m}$  of implanted strip width at a  $V_{\text{bias}} = 400 \text{ V}$ . For an AMS sensor, the upper limit is  $35 \text{ pA}/\text{cm}$  per  $\mu\text{m}$  of implanted strip width (equivalent with  $2 \text{ nA}$ ) at  $V_{\text{bias}} = 80 \text{ V}$  for the p-side and respectively  $70 \text{ pA}/\text{cm}$  per  $\mu\text{m}$  of implanted strip width (equivalent with  $20 \text{ nA}$ ) for the n-side at the same  $V_{\text{bias}}$ .

Examples of electrical set-up configurations for the  $I_{\text{ss}}$  measurement of a single-sided and p- and n-side double-sided sensor are presented in Fig. 9a), b), and respectively c).

The set-up presented in Fig. 9b) and c) helps also to identify the shorts between the neighboring strips (e.g. for the p-side, small voltage drop (e.g.  $50 \text{ mV}$ ) is applied between the measured strip and adjacent ones). Typical  $I_{\text{ss}}$  scans of a CMS single-sided sensor (768 strips) and p-side (1284 strips) and n-side (384 strips) of an AMS double-sided sensor are presented in Fig. 10a), b) and respectively c).

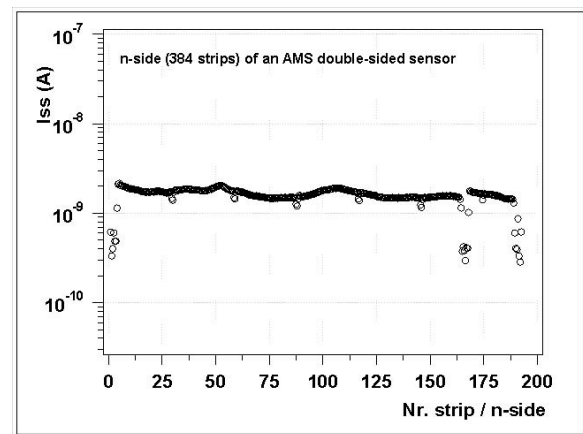
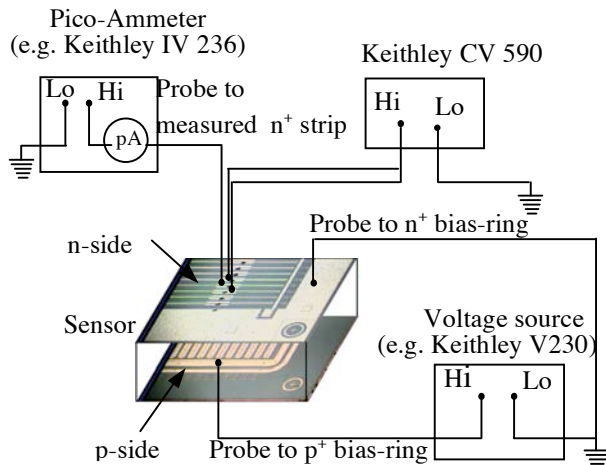
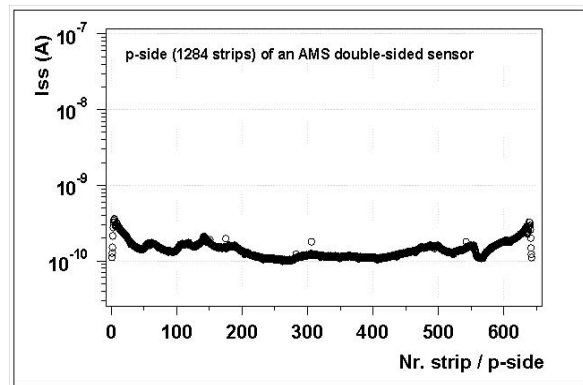
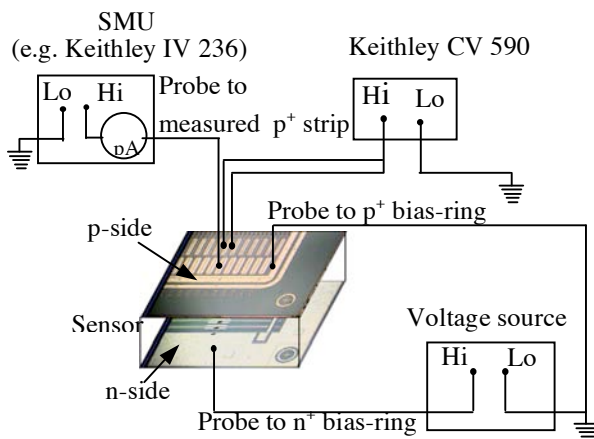
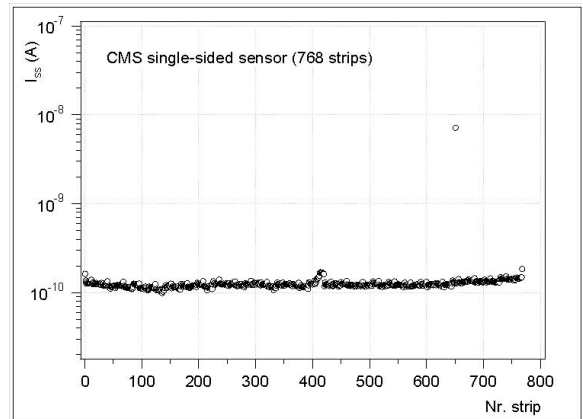
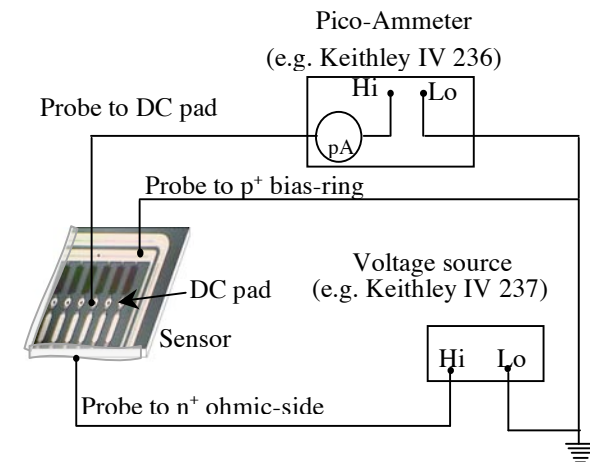


**FIG. 9a):** Example of electrical set-up configuration for the  $I_{ss}$  measurement of a single-sided sensor; **b)** the same as a) but for p-side of a double-sided sensor; **c)** the same as a) but for the n-side of double-sided sensor

**FIG. 10a):** Typical  $I_{ss}$  scan of a CMS single-sided sensor (768 strips); **b)** the same as a) but for the p-side (1284 strips) and **c)** for the n-side (384 strips) of an AMS double-sided sensor

#### 4.2.2 Bias resistance

As mentioned in the Section 2, two methods are usually used to carry uniformly the bias voltage from the bias-ring to all the strips: the poly-silicon resistances and the punch-through. The values of both poly-silicon resistance  $R_{\text{poly}}$  (for poly-silicon biasing) and the bias-ring to strip resistance  $R_{\text{br-s}}$  (for punch-through biasing) are determined by fabrication process and they should be sufficiently high to guarantee low noise (see discussion at the beginning of the Section 4).

For example, each  $R_{\text{poly}}$  value for a CMS sensor is required to be  $1.5 \pm 0.5 \text{ M}\Omega$ . For punch-through biasing, usually the following relation holds  $R_{\text{br-s}} I_{\text{ss}} \approx V_{\text{drop}}$ , where the  $V_{\text{drop}}$  is the voltage drop between the strip and the bias-ring. The  $V_{\text{drop}}$  is set to few volts (e.g.  $\sim 2\text{V}$  for AMS sensors). Therefore, the  $R_{\text{br-s}}$  varies usually in the range  $1 \div 10 \text{ G}\Omega$ .

Electrical set-up configurations which can be used for the measurement of  $R_{\text{poly}}$  and  $R_{\text{br-s}}$  are presented in Fig.11 and respectively Fig.12. The usual procedure for determination of the each strip resistor is to apply different voltages  $V$  across the resistor and to measure the resulting current  $I$  (using an SMU as indicated in Figs.11 and 12). For example,  $(-5\text{V} \div 5\text{V})$  and  $(-250\text{mV} \div 250\text{mV})$  voltage ranges have been used for the measurement of  $R_{\text{poly}}$  of the CMS sensors and  $R_{\text{br-s}}$  of the AMS sensors respectively. The resistor value for each strip is then determined from the slope of the linear fit of the corresponding IV curve.

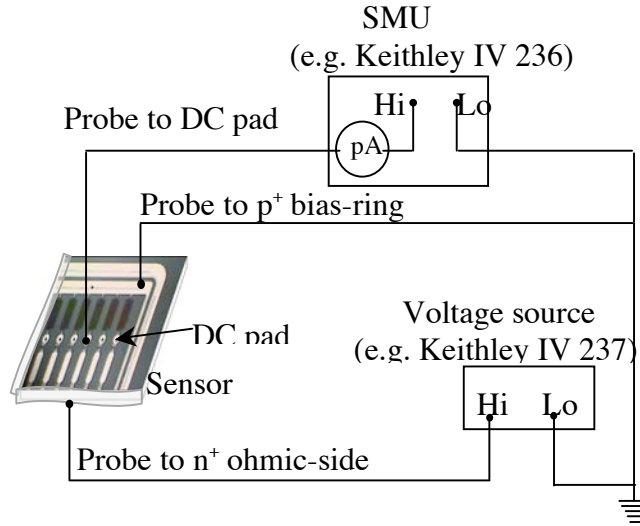


**FIG. 11:** Example of electrical set-up configuration for the  $R_{\text{poly}}$  measurement for a single-sided sensor biased through poly-silicon resistors

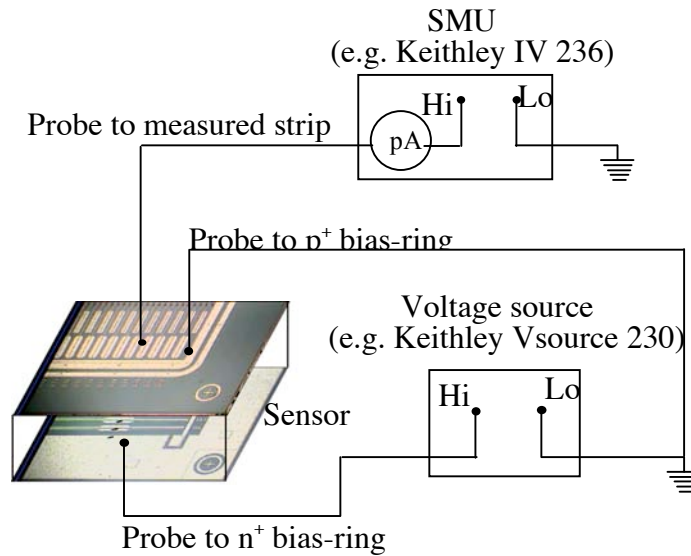


**FIG. 12:** Example of electrical set-up configuration for the  $R_{s-br}$  measurement for a double-sided sensor biased through punch-through method

Fig.13 presents a graph of measured currents across  $R_{poly}$  as a function of different applied voltages for few strips of a CMS sensor. A completely  $R_{poly}$  scan for a CMS sensor with 512 strips is presented in Fig.14. One should note the good uniformity and the stability of the resistance assured by the poly-silicon resistance design.

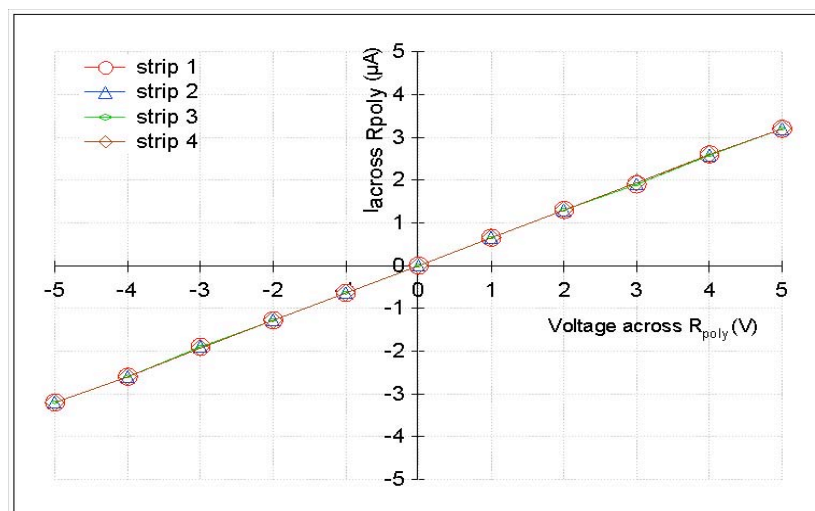


**FIG. 13:** Example of current across  $R_{poly}$  vs applied voltages for few strips of an CMS sensor

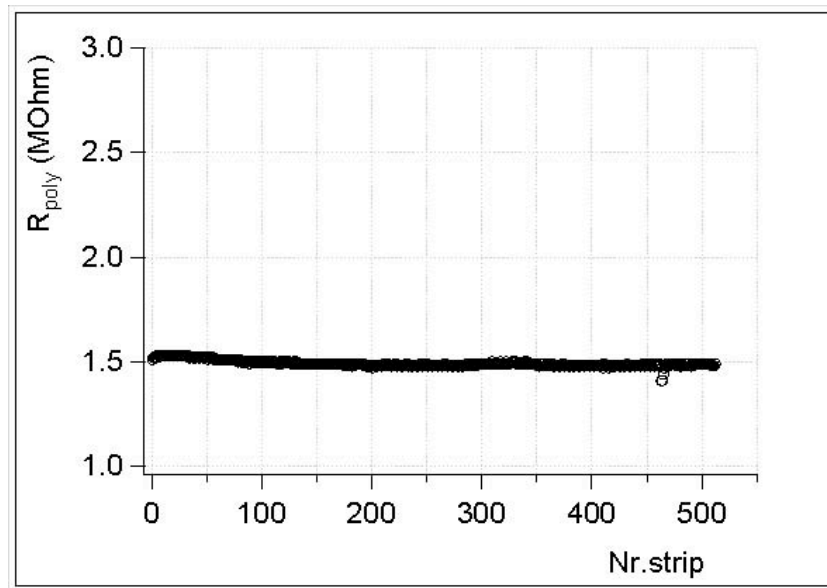


**FIG. 14:** Typical  $R_{\text{poly}}$  scan for a CMS sensor with 512 strips

#### 4.2.3 Coupling capacitance and dielectric current (AC coupling)

As stated in the Section 2, the AC-coupling method is used to protect the read-out electronics from high levels of the sensor leakage current. This method consists of an arrangement of oxides and nitrides layers grown between the implanted strips and corresponding aluminum strip that lies over them. The capacitance determined by these layers is called coupling capacitance  $C_{\text{ac}}$ .

The  $C_{\text{ac}}$  measurement of all strips is usually performed to provide a measure of the uniformity of the oxide layer as well as to give us confidence about the resulting homogeneity in the charge collection (the  $C_{\text{ac}}$  influences the signal strength to the read-out electronics). The  $C_{\text{ac}}$  values should be maximized to assure high efficiency charge collection. For example, the  $C_{\text{ac}}$  for a CMS sensor is required to be  $1.2 \div 1.3$  pF/cm per  $\mu\text{m}$  of implanted width strip.

An example of electrical set-up configuration for the measurement of  $C_{\text{ac}}$  is presented in Fig.15. This set-up helps also to detect metal shorts between neighboring strips: the capacitance is measured between three adjacent DC pads shorted together and the corresponding central AC pad. In this way, when a short occurs between two of three measured capacitors, the resulting value corresponds to two capacitors in parallel and it is twice the correct one.

Typical  $C_{\text{ac}}$  scans for two CMS sensors AC-coupled to the read-out electronics are presented in Fig. 16a) and b). The different mean  $C_{\text{ac}}$  values of these sensors are explained by their different designs: the sensor presented in Fig.16a) is characterized by a strip length of 11.6 cm, a width of the implanted strip of  $30 \mu\text{m}$  and a pitch of  $120 \mu\text{m}$  while the sensor presented in Fig.16b) is characterized by a strip length of 11.6 cm, a width of the implant strip of  $20 \mu\text{m}$  and a pitch of  $80 \mu\text{m}$ .

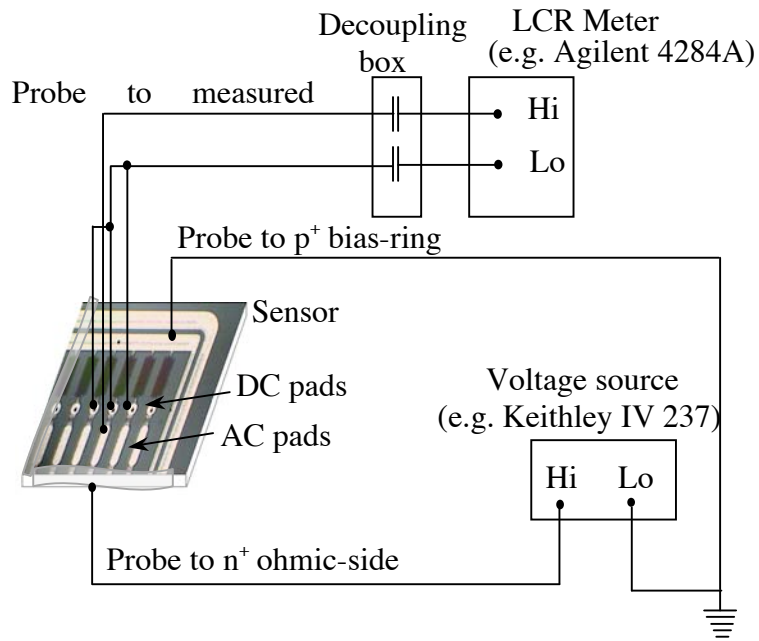


**FIG. 15:** Example of electrical set-up configuration for the  $C_{ac}$  measurement for sensors with strips AC-coupled to the read-out electronics

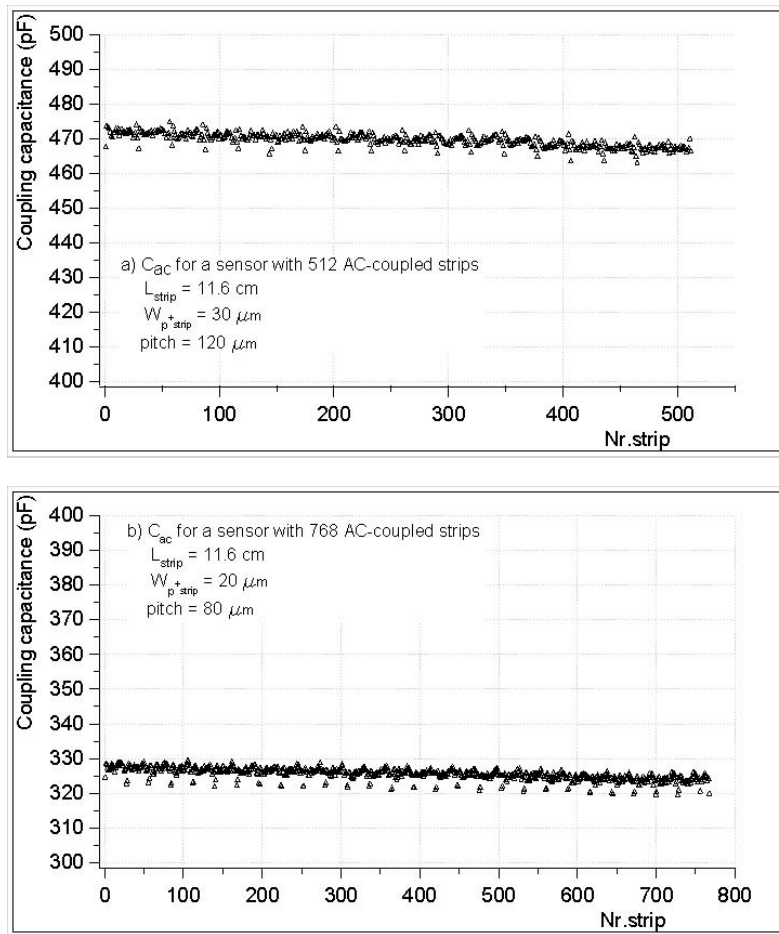


**FIG. 16a) and b):** Examples of  $C_{ac}$  scans for two CMS sensors with different characteristics designs

A perfect oxide insulator over the large surface of a silicon micro-strip sensor is difficult to be produced and usually different defects appear during processing. The most common defect is called “pinhole” and it represents a short (or low resistivity connection) through the oxide. A strip with pinhole is supposed to not be connected because the electronics may be damaged by the high voltage from the strip through the broken capacitor. Therefore, the number of such defects should be as small as possible.

The presence of pinholes is identified measuring the dielectric current  $I_{\text{diel}}$  through the oxide layer. For a strip with good capacitor the  $I_{\text{diel}}$  equals the noise of the set-up ( $\sim \text{pA}$ ), while a strip presenting a pinholes has much higher  $I_{\text{diel}}$  value (usually  $O(\mu\text{A})$ ).

An electrical set-up configuration which can be used for the measurement of  $I_{\text{diel}}$  is presented in Fig.17. A voltage drop is applied between the DC and AC pads of the strip under test (e.g. 10 V were applied in the case of the CMS sensors) and the current through oxide is measured.

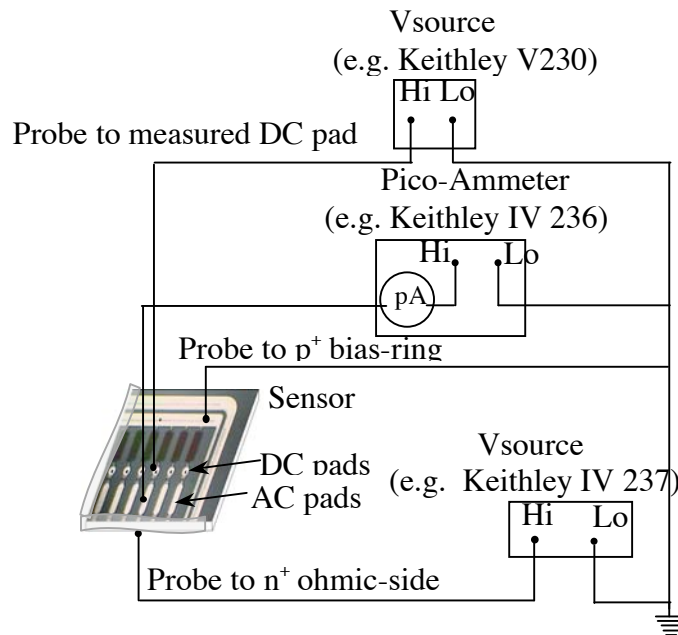


**FIG. 17:** Example of electrical set-up configuration for the  $I_{\text{diel}}$  measurement for sensors with strips AC-coupled to the read-out electronics

A typical  $I_{\text{diel}}$  scan for a CMS sensor with 512 AC-coupled strips is presented in Fig.18. A strip with high  $I_{\text{diel}}$  (pinhole) can be identified.

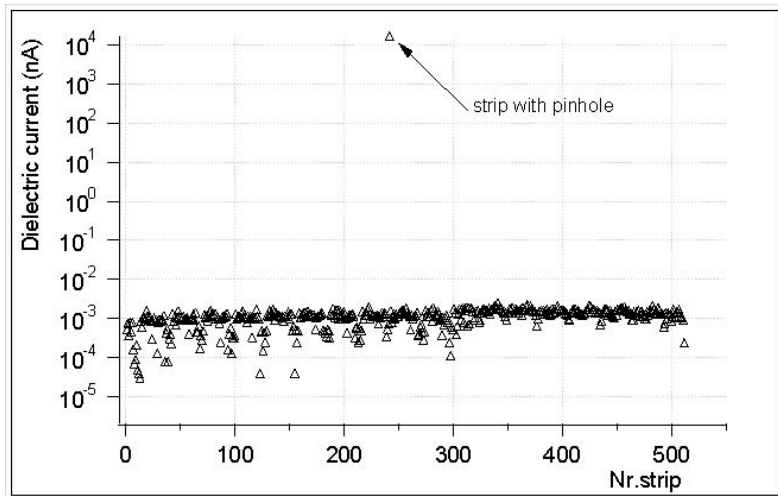


**FIG. 18:** Typical  $I_{\text{diel}}$  scan for a CMS sensor with 512 AC-coupled strips. A strip with high  $I_{\text{diel}}$  (pinhole) can be identified.

## 5 CONCLUSION

We presented an overview of the electrical characterization of silicon micro-strip sensors. Mainly, a description of strip parameters which contribute to the noise of the corresponding electronics channels (single strip leakage current, biasing resistance, dielectric current) as well as global parameters (total leakage current and total capacitance) have been described. General requirements on the hardware set-up recommended for an accurate characterization of these parameters have been also illustrated. These measurements may be generalized to any silicon micro-strip sensor geometry.

This work was based on five years experience accumulated during electrical qualification tests performed on micro-strip sensors fabricated for CMS and AMS experiments. Essentially, the electrical parameters of  $\sim 4000$  double-sided AMS sensors and  $\sim 6000$  single-sided CMS sensors have tested and analyzed.

## 6 REFERENCES

- (1) CMS Tracker TDR, CERN/LHCC 98-6 CMS TDR 5, 1998.
- (2) M. Aguilar et al, by AMS collaboration, Phys. Rept. **366**, 331, (2002).
- (3) G. Calefato et al, Nucl. Instr. & Meth. in Phys. Res. **A 476**, 744, (2002) .
- (4) J. Kemmer, Nucl. Instr. & Meth. in Phys. Res. **169**, 499, (1980) .
- (5) M. Caccia et al, Nucl. Instr. & Meth. in Phys. Res. **A 260**, 124, (1987) .
- (6) L. Evensen et al, IEEE Trans. Nucl. Sci. **35**, 428, (1988) .
- (7) Y.Iwata et al, IEEE Trans. Nucl. Sci. **45**, 303, (1998) .
- (8) D. Pitzl et al, Nucl. Phys. B (Proc. Suppl.) **23A**, 340, (1991) .
- (9) J. Kemmer, G. Lutz, Nucl. Instr. & Meth. in Phys. Res. **A273**, 588, (1988) .
- (10) G. Lutz, Semiconductor Radiation Detectors, Device Physics, Springer 1999, Ch.7.
- (11) N. Bacchetta et al, Nucl. Instr. & Meth. in Phys. Res. **A342**, 39, (1994).
- (12) J. -L. Agram et al, Nucl. Instr. & Meth. in Phys. Res. **A 517**, 77, (2004).
- (13) N. Dinu, E. Fiandrini, Proc. 20<sup>th</sup> IEEE Instr. & Meas. Tech. Conf., Vail, Colorado, USA 20-22 May 2003.
- (14) M. Wood et al, Conf. Record of the 1991 IEEE Nucl. Sci. Symp. & Medical Imag. Conf., Santa Fe, 2-9 Nov. 1991.
- (15) R. Sonnenblick et al, Nucl. Instr. & Meth. in Phys. Res. **A310**, 189, (1991).
- (16) E. Nygard et al, Nucl. Instr. & Meth. in Phys. Res. **A301**, 506, (1991).
- (17) P. F. Ermolov et al, Instr. & Exp. Tech. **45**, 194, (2002).
- (18) A. S. Grove, Physics and Technology of Semiconductor Devices, John Wiley & Sons, 1967, Ch. 6.